The role of calcium response in regulation and maintenance of secretory function in salivary glands

(唾液腺の分泌機能の調節と維持におけるカルシウム応答の役割)

日本大学松戸歯学研究科細胞機能制御学専攻

櫻井　甫

(指導　吉垣純子)

Abstract

Saliva regulates the environment of the oral cavity and hyposecretion of saliva results in serious caries and periodontitis. In salivary glands, muscarinic stimulation evoke elevation of intracellular Ca^{2+} concentration, which leads to fluid secretion of saliva. Calcium response in salivary acinar cells is considered to be important for regulation of saliva secretion.

In this study, we examined calcium response of salivary gland cells isolated from two strain mice. C57BL/6CrSlc (B6) and C3H/HeSlc (C3H) have been reported to have different sensitivities to caries. C3H, which has a lower sensitivity to caries, have a higher ability to secrete saliva compared with B6. In this study, we compared Ca^{2+} mobilization in submandibular gland cells of the two strains. Muscarinic stimulation evoked rapid increase and sustained elevation of intracellular Ca^{2+}, which are due to release of Ca^{2+} from intracellular pool and store-operated Ca^{2+} entry (SOCE), respectively. When cells were stimulated by 1 μM carbachol, there is no significant difference between the peaks of Ca^{2+} response in the two strains. However, the sustained phase of Ca^{2+} elevation tends to be higher in C3H than in B6. Following stimulation with 10 μM carbachol results in higher peak and sustained phase in C3H compared to in B6. Ca^{2+} elevation induced by the inhibitor of endoplasmic reticular Ca^{2+} pump thapsigargin in Ca^{2+}-free medium was higher in C3H than in B6. In contrast, there was no difference in SOCE observed by addition of extracellular Ca^{2+} after depletion of Ca^{2+} by thapsigargin between the two strains. In addition, expression levels of genes that are involved in SOCE were not different between the two strains. These results suggest that the different response of Ca^{2+} elevation is due to the difference in capacity of intracellular Ca^{2+} pool.

Next, we examined effects of a reactive oxygen scavenger on the salivary gland function. We previously reported that the process of cell isolation from parotid glands triggers stress signaling mediated by Src and p38 MAP kinase (p38), which led to dedifferentiation of acinar cells. An NADPH oxidase inhibitor suppressed activation of Src and p38, suggesting that reactive oxygen species initiated the dedifferentiation signal. In this study, we examined the effect of a free radical scavenger, 3-methyl-1-phenyl-2-pyrazolin-5-one (also called MCI-186 or edaravone), on activation of the stress signal and the secretory functions of parotid acinar cells. The results showed that activation of p38 during cell isolation was suppressed by the addition of MCI-186. The retention of the activity of amylase, a major salivary protein, and the number of amylase-containing secretory granules was improved after isolation and culture in the presence of MCI-186. In addition, calcium elevation upon stimulation with a muscarinic agonist was higher in MCI-186-treated cells than in untreated cells.

Since submandibular gland cells of C3H, which has a higher ability to secrete saliva, showed a higher calcium response upon strong muscarinic stimulation, capacity of intracellular Ca^{2+} pool may determine secretory rate of saliva. To keep secretory function of salivary glands, maintenance of high calcium response is essential and the superoxide scavenger MCI-186 is a promising agent for the prevention of salivary gland dysfunction.

Introduction

Saliva is essential for maintenance of the oral environment. Fluid and ion secretion of saliva is regulated by parasympathetic activation. Muscarinic agonists induce synthesis of inositol triphosphate (IP_3) and consequent activation of IP_3 receptors (IP_3Rs) located in the endoplasmic reticulum (ER). Release of Ca^{2+} from the ER via IP_3Rs is essential for fluid secretion of salivary glands (1). Elevation of intracellular Ca^{2+} concentration ($[Ca^{2+}]_i$) activates Ca^{2+}-dependent Cl^- channels located in the luminal membrane, which causes efflux of Cl^- to the lumen (2-4). Electrochemical gradient produced by Cl^- induces transport of Na^+ from blood plasma to the lumen through tight junctions. The resulting osmotic gradient for NaCl evokes transepithelial movement of water (5).

In addition of release of Ca^{2+} from the ER, depletion of ER-stored Ca^{2+} leads to activation of plasma membrane Ca^{2+} channels that mediate influx of Ca^{2+} from the extracellular fluid into cells, which is called store-operated Ca^{2+} entry (SOCE) (6). The magnitude of SOCE is also one of the factors that determine the saliva flow rate (7). As the Ca^{2+} sensor of the intracellular compartments and plasma membrane Ca^{2+} channel, stromal interaction molecule (STIM) and Orai were identified, respectively (8-10). It is widely accepted that both Ca^{2+} release from the ER and SOCE in salivary acinar cells regulate saliva fluid secretion.

Therapeutic radiation for head and neck cancers causes apoptosis and atrophy of acinar cells in salivary glands. Thus, in many patients, there is an irreversible decrease in saliva after radiotherapy. In addition, chronic inflammatory conditions, such as Sjögren's syndrome, also induce tissue damage and decrease parenchymal cells. The decrease of saliva and consequent dry mouth leads to severe caries and periodontitis. Approaches to protect

salivary gland cells from this damage and to maintain the secretory functions are greatly needed.

In this study, we searched the factors that regulate and maintain the secretory function of saliva. First, we investigated the mechanism that determines the amount of saliva in the two strain mice, which have different abilities to secrete saliva. Next, we examined the effect of MCI-186, a scavenger of reactive oxygen species, on the maintenance of salivary gland functions.

Research 1: Difference in calcium mobilization between two strains of mice that have different abilities to secrete saliva

Introduction

Two mouse strains, C57BL/6CrSlc (B6) and C3H/HeSlc (C3H), have been reported to have different sensitivities to caries. Oral inoculation of *Streptococcus mutans* resulted in caries with a higher rate in B6 than in C3H (11). C3H, which has a lower sensitivity to caries, have a higher ability to secrete saliva compared with B6 (12). Although saliva flow rate may affect caries susceptibility, the reason that causes the difference in saliva flow rate has not been resolved. Intracellular Ca^{2+} concentration regulated by muscarinic stimulation is considered essential for fluid secretion. Thus, in the second study, in order to find factors that determine the saliva flow rate, we compared Ca^{2+} mobilization and gene expression involved in SOCE in submandibular gland cells of the two strains.

Materials and Methods

Preparation of submandibular gland cells

All animal experiments were carried out in accordance with institutional and national guidelines for the care and use of experimental animals and was approved by the Experimental Animal Committee of the Nihon University School of Dentistry at Matsudo (AP16MD020). Submandibular glands were removed from male B6 and C3H mice under anesthesia with a combination of 0.3 mg/kg of medetomidine, 4.0 mg/kg of midazolam, and

5.0 mg/kg of butorphanol. The cells were isolated from submandibular glands as reported previously (13). Briefly, finely minced glands were digested with collagenase and hyaluronidase in Hanks' balanced salt solution containing 20 mM HEPES-NaOH, pH7.4 and 0.5% bovine serum albumin at 36°C for 30 min.

Measurement of intracellular Ca^{2+} mobilization

Isolated submandibular gland cells were loaded with 2 μM fura-2 AM (Thermo Fisher) in loading buffer (10 mM HEPES-NaOH, pH 7.4, 140 mM NaCl, 5 mM KCl, 1 mM $MgCl_2$, 2.5 mM $CaCl_2$, 10 mM glucose, 1.25 mM probenecid). When thapsigargin was used, the cells were washed and suspended with Ca^{2+}-free buffer. The fluorescence of the fura-2-loaded cells was measured by using CAF-110 (Jasco, Tokyo, Japan) with excitation at 340 and 380 nm, and emission at 510 nm. Elevation of the intracellular Ca^{2+} concentration was evaluated as the increase in the ratio of fluorescence intensities at 340 nm and 380 nm (F340/F380). The increase in F340/F380 before and at times indicated in the figure legends after stimulation was shown as ΔF340/F380, which reflects increase in intracellular Ca^{2+} concentration.

RNA preparation and real time RT-PCR analysis of mRNA expression

Total RNA was isolated from the submandibular gland cells using the Qiazol Lysis reagent and RNeasy Mini kits (Qiagen, Hilden, Germany). Amounts of RNA were quantified by measuring the absorbance at 260 nm. Expression levels were determined with One Step TB Green PrimeScript PLUS kit (Takara Bio, Kusatsu, Japan). Gapdh was used as a reference. Primer pairs for amplification of STIM1, STIM2 and Orai1 were as follows: *Stim1*: forward 5'- CAG AAG TGT ACA ACT GGA CTG TG -3', reverse 5'- GGT TAC TGC TAG CCT

TGG CAT G -3' with a predicted size of 130 bp; *Stim2*: forward 5'- ATG CAG AGC AGG AAC TGG AG -3', reverse 5'- CGT GTG TTA GCT GAA GCC ATT TC -3' with a predicted size of 119 bp; *Orai1*: forward 5'- GCT AAG GAG TAA GGA GTT TGA G -3', reverse 5'- GAA TGG GGA CAG TTG CTC TC -3' with a predicted size of 96 bp. PCR products were evaluated by melting curve analysis according to the manufacturer's instructions and by examining the sizes of the PCR products separated on 2.0% agarose gels. Relative RNA equivalents for each sample were obtained by normalizing to GAPDH levels. Each sample was run in duplicate to determine the sample reproducibility, and the average relative RNA equivalents per sample pair were used for further analysis.

Statistical analyses

All values are reported as means ± SEM. Statistical analyses of the differences in the means of experimental pairs were evaluated by an unpaired *t*-test. The *P* values obtained are indicated in the figure legends when statistically significant.

Results

Comparison of Ca^{2+} response induced by carbachol

Muscarinic stimulation increases the intracellular Ca^{2+} concentration ($[Ca^{2+}]_i$), which is essential for fluid secretion of saliva. We examined Ca^{2+} response in submandibular gland cells prepared from the two strains of mice. The values of basal F340/F380 ratio of B6 and C3H before stimulation were 0.745 ± 0.027 and 0.788 ± 0.021, respectively. When cells were

stimulated by 1 μM carbachol (CCh), there is no significant difference between the peaks of Ca^{2+} elevation in the two strains (Fig. 1.1A). However, the sustained phase at 2 min after addition of CCh was higher in C3H than in B6 although there is no significant difference (Fig. 1B). ΔF340/F380 in the sustained phase in C3H was kept 71.4% ± 8.3 of the peak while that of B6 was only 53.4% ± 9.3. In addition, the peak response and sustained phase induced by additive stimulation with 10 μM CCh were also higher in C3H than in B6 (Fig. 1A and C).

Expression levels of genes involved in store-operated calcium entry

Sustained phase of Ca^{2+} elevation induced by muscarinic stimulation is affected by SOCE. Because the sustained phase of Ca^{2+} level induced by 1 μM CCh in C3H tends to be higher than in B6, expression levels of genes that are involved in SOCE such as STIM1, STIM2 and Orai1 in submandibular gland cells were quantified. Although the expression of all the three genes was detected in submandibular gland cells of the two strains, there is no significant difference in expression levels between the two strains (Fig. 1.2).

Comparison of Ca^{2+} elevation induced by thapsigargin

We used thapsigargin, an inhibitor of ER Ca^{2+} ATPase, to examine the capacity of intracellular Ca^{2+} pool and SOCE. When thapsigargin was added to the cells suspended in Ca^{2+}-free extracellular buffer, Ca^{2+} leaking out from the intracellular pools was no longer recovered, so $[Ca^{2+}]_i$ gradually increased (Fig. 1.3A and B). We found that the increase in $[Ca^{2+}]_i$ induced by thapsigargin was larger in C3H than in B6 (Fig. 1.3B and C). Addition of extracellular Ca^{2+} after depletion of intracellular pool induced rapid and large increase in $[Ca^{2+}]_i$, which corresponds to SOCE. The magnitude of SOCE was not different between the

two strains (Fig. 1.3A).

Discussion

In salivary glands, primary saliva is produced as isotonic fluid in acini. The primary saliva is then modified by removal and addition of ions during passing in the ducts without absorption and secretion of water. Therefore, the amount of the primary saliva produced in acini determines saliva flow rate. Increase of $[Ca^{2+}]_i$ in acinar cells is the primary trigger for salivary fluid secretion. Ion transport initiated by increase of $[Ca^{2+}]_i$ makes transepithelial salt gradients, which evokes water movement from blood to the acinar lumen (5). Therefore, understanding the molecular machinery to regulate $[Ca^{2+}]_i$ is necessary to clarify the mechanism for regulation of saliva flow rate.

Muscarinic stimulation causes rapid increase and sustained elevation of $[Ca^{2+}]_i$. The two phases of Ca^{2+} mobilization are considered to depend on release from intracellular pool and influx from extracellular space, respectively. In this study, there was no difference in the peak response upon stimulation with 1 μM CCh between the two strains. This process is dependent on activation of muscarinic receptors and IP_3Rs, which may be comparable in both strains. A previous study showed that gene expression levels of muscarinic receptors in the two strains were comparable (12), which also supports this inference. In contrast, the sustained phase of Ca^{2+} mobilization tends to be higher in C3H than in B6. Moreover, the peak response to additional stimulation with 10 μM CCh rose higher than the first response with 1 μM CCh in C3H, while response to 10 μM CCh was lower than that of 1 μM in B6.

We also measured the effect of thapsigargin on the change of $[Ca^{2+}]_i$. Thapsigargin

inhibits the ER Ca^{2+} pump that plays a role in recovery of Ca^{2+} from cytosol to the ER Ca^{2+} pool (14). Addition of thapsigargin causes leak of Ca^{2+} from the ER and consequentially increases $[Ca^{2+}]_i$. In this study, the elevation of $[Ca^{2+}]_i$ induced by thapsigargin was higher in C3H than in B6. Combined with the results of response to CCh, it is likely that the capacity of intracellular Ca^{2+} pool was larger in C3H than in B6. Strong and long stimulation may lead to depletion of the Ca^{2+} pool and resulting smaller response in B6. There is a possibility that the difference in capacity of Ca^{2+} pool is one of the reasons of the difference in Ca^{2+} response between the two strains.

We observed SOCE caused by addition of extracellular Ca^{2+} after depletion of intracellular pool by thapsigargin. There was no significant difference in rates and amounts of Ca^{2+} influx between the two strains. In addition, the expression levels of STIMs and Orai1 mRNAs were not significantly different between the two strains. These results suggest that factors other than SOCE is the cause of the difference in the sustained phase of Ca^{2+} mobilization.

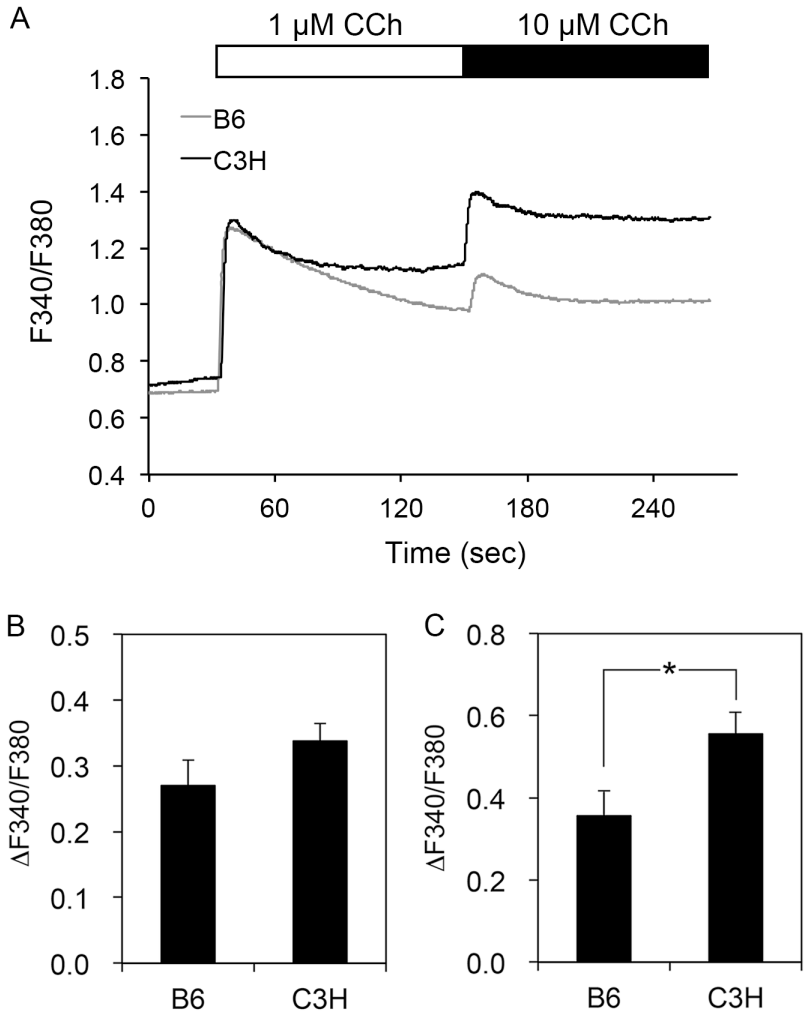

Fig. 1.1 Comparison of Ca^{2+} responses in submandibular gland cells of C3H and B6. A. Time course of Ca^{2+} response to 1 and 10μM CCh. The values are shown as the ratio of the fluorescence intensities at 510 nm following excitation at 340 nm and 380 nm (F340/F380). B. Comparison of the increase in F340/F380 (ΔF340/F380) at sustained phase after stimulation by 1 μM CCh between the two strains. The values (ΔF340/F380) are shown as the difference from the basal level before stimulation and at 2 min after stimulation by 1 μM CCh. Although there is no significant difference between the two strains, ΔF340/F380 of the sustained phase in C3H tends to be higher than in B6 (n = 8). C. Comparison of ΔF340/F380 between the basal level and the peak response to 10 μM CCh between the two strains. The peak response was significant higher in C3H than in B6 (*$P < 0.05$; unpaired *t*-test, n = 8).

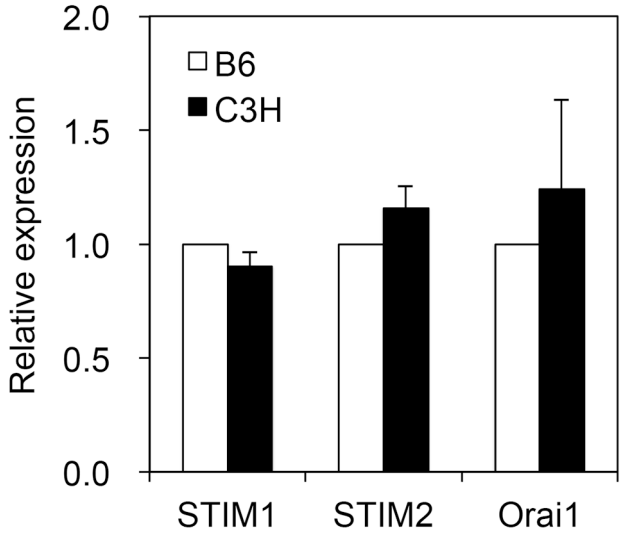

Fig. 1.2 Comparison of expression levels of SOCE-related genes between the two strains. Expression levels of STIM1, STIM2 and Orai mRNAs in C3H are shown as relative values to those in B6. There was no significant difference between the two strains.

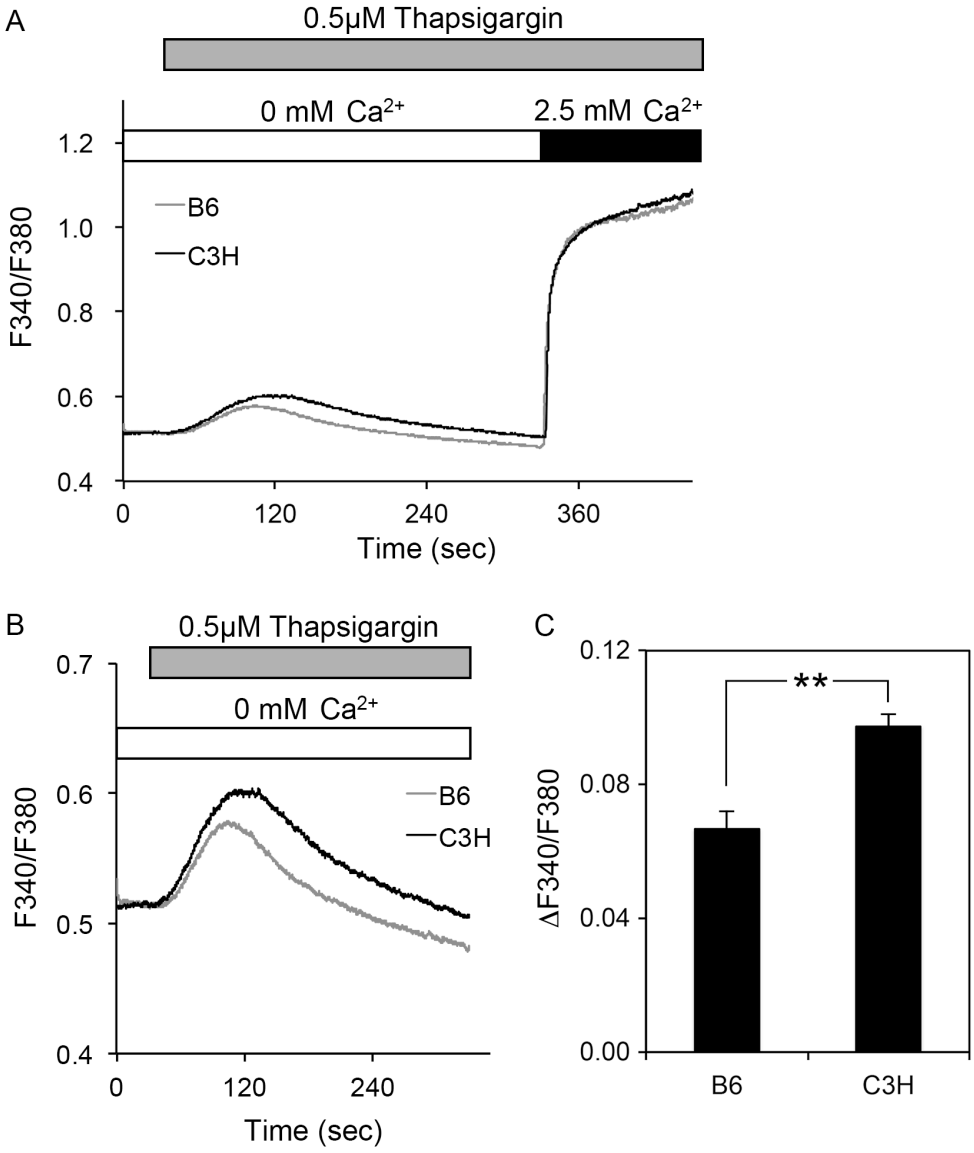

Fig. 1.3 Effect of thapsigargin on $[Ca^{2+}]_i$ in submandibular gland cells. A. Time course of changes in $[Ca^{2+}]_i$. Cells suspended in Ca^{2+}-free buffer (0 mM Ca^{2+}) were treated with 0.5 μM thapsigargin for 5 min, and then, Ca^{2+} was added to the extracellular buffer (final concentration of 2.5 mM). B. A part of Fig. 3A is shown. Scale of y-axis was changed to smaller range to emphasize the increase of $[Ca^{2+}]_i$. C. The increase in F340/F380 (ΔF340/F380) between the basal level and the peak after addition of thapsigargin in the absence of extracellular Ca^{2+}. ΔF340/F380 induced by thapsigargin was significantly higher in C3H than in B6 (*$P < 0.05$; unpaired *t*-test, n = 8).

Research 2: Suppression of parotid acinar cell dysfunction by the free radical scavenger 3-methyl-1-phenyl-2-pyrazolin-5-one

Introduction

To study the mechanism that maintains the secretory functions of salivary acinar cells, we established a system for primary culture of parotid acinar cells that maintained the capacity to generate secretory granules (SGs) and stimulus-dependent secretion of salivary proteins (15). However, this capacity gradually decreased, and the expression of differentiation markers changed during culture (16); the expression levels of acinar markers, such as amylase and aquaporin-5, decreased, while that of ductal markers and mesenchymal markers increased. Inhibitors of Src and p38 MAP kinase (p38) suppressed these changes and increased the expression of acinar marker proteins. These results suggest that the Src-p38 signaling pathway plays a role in triggering cell differentiation for survival from cellular stress (17). Diphenyleneiodonium (DPI), an NADPH oxidase inhibitor, suppressed activation of Src and p38 (18). Therefore, reactive oxygen species (ROS) may be generated during cell isolation and activate Src. Oxidative stress has been suggested to be involved in the development of Sjögren's syndrome (19) and hyposalivation after γ-irradiation (20).

However, using DPI to suppress stress signals carries a risk of side effects, because DPI also has inhibitory activities against other enzymes, such as nitric oxide synthetases. In this study, we examined the effect of 3-methyl-1-phenyl-2-pyrazolin-5-one, also called MCI-186 or edaravone, which has been approved for the treatment of the acute phase of brain infarction and amyotrophic lateral sclerosis (21, 22) on the activation of dedifferentiation signaling and the secretory functions of parotid acinar cells.

Materials and Methods

Materials

Rabbit polyclonal anti-amylase and mouse monoclonal anti-occludin antibodies were purchased from Merck (Darmstadt, Germany). Mouse monoclonal anti-p38 and rabbit polyclonal anti-phosphorylated p38 antibodies were purchased from BD Biosciences (Sparks, MD, USA) and R&D systems (Minneapolis, MN, USA), respectively. MCI-186 was purchased from Cayman Chemical Company (Ann Arbor, MI, USA). Culture medium and supplements were purchased from Thermo Fisher Scientific (Waltham, MA, USA).

Preparation and culture of isolated acinar cells

All animal experiments were carried out in accordance with institutional and national guidelines for the care and use of experimental animals and were approved by the Experimental Animal Committee of the Nihon University School of Dentistry at Matsudo (AP15MD018). Parotid glands were removed from male Sprague-Dawley rats (weighing 150 - 200 g) under inhalation anesthesia with 3% sevoflurane. Acinar cells were isolated from the glands as described previously (23). Briefly, finely minced glands were digested with collagenase and hyaluronidase in isolation buffer (Hanks' balanced salt solution containing 20 mM HEPES-NaOH, pH7.4) in the absence or presence of MCI-186. The isolated cells were diluted to 0.3 mg/ml protein in Waymouth's medium containing 10% rat serum, ITS-X supplement, 1 μM hydrocortisone, 100 U/ml penicillin, 0.1 mg/ml streptomycin and 10 nM

cystatin, and were cultured at 37°C in 5% CO_2. The medium was changed 1 day after cell isolation. MCI-186 was dissolved in dimethylsulfoxide (DMSO) to a concentration of 50 mM as a stock solution and was diluted 1:1000 to a final concentration of 50 μM for use. The same volume of DMSO was added to the control medium (final, 0.1%).

SDS-PAGE and immunoblotting analysis

Cells were lysed with 20 mM HEPES-NaOH (pH7.4) containing 0.1% Triton X-100 and 1× Complete Protease Inhibitor Cocktail (Roche, Basel, Switzerland). The proteins were separated by SDS-PAGE and transferred to Hybond-LFP membranes (GE Healthcare, Chicago, IL, USA). The membranes were blocked at room temperature for 1 h in Blocking reagent (GE Healthcare) and probed with the primary antibodies. Immunoreactivity was determined by using ECL-Plex (GE Healthcare), and images are acquired using Typhoon Trio (GE Healthcare). The intensities of the immunoreactivities were quantified by using ImageQuantTL software (GE Healthcare). The intensity of immunoreactivity in MCI-treated sample was normalized to that in untreated sample in the same blotting membrane. After the normalized values of total and phosphorylated p38 were acquired, the ratio of the phosphorylated form to total p38 was calculated in each experiment.

Immunofluorescence microscopy of cultured acinar cells

Acinar cells were plated on collagen I-coated dishes (Iwaki, Tokyo, Japan) and were cultured for 3 days. Then, the cells were treated with 10% formalin in phosphate-buffered saline (PBS) for 5 min and subsequently treated with 0.2% Triton X-100 in PBS for 10 min. After blocking with bovine serum albumin and preimmune goat IgG, the cells were labeled with the primary

antibodies, followed by the respective Alexa Fluor-labeled secondary antibodies. Images were acquired using a 100× 1.46 αPlan-Apochromat oil objective lens on an LSM-510 laser confocal microscope (Carl Zeiss, Oberkochen, Germany). Optical sections were taken along the z-axis at 0.5 μm intervals. The number of granules was counted by spot analysis with Imaris software (Bitplane, Zurich, Switzerland). Amylase-positive spots were selected with a threshold diameter of 0.5 μm. When the software did not count the spots because of overcrowding, we excluded them because we could not judge whether they were granules.

Amylase release assay

Cells cultured in dishes were incubated with release buffer (20 mM HEPES-NaOH, pH 7.4, 128 mM NaCl, 4 mM KCl, 1.2 mM $MgCl_2$, 1 mM $CaCl_2$, 1 mM NaH_2PO_4, 5 mM hydoxybutyrate) in the absence or presence of 10^{-6} M isoproterenol (Iso) at 37°C for 15 min (15). After incubation, the solution was removed, and the remaining cells were harvested. Amylase activity was measured by a previously reported method One unit of amylase was defined as the quantity of enzyme that liberates 1 mg of maltose for 1 min at 30°C.

Measurement of intracellular Ca^{2+} mobilization

Isolated parotid acinar cells were loaded with 2 μM fura-2 AM (Thermo Fisher) in loading buffer (10 mM HEPES-NaOH, pH 7.4, 140 mM NaCl, 5 mM KCl, 1 mM $MgCl_2$, 2.5 mM $CaCl_2$, 10 mM glucose, 1.25 mM probenecid, and 0.2% bovine serum albumin) at 37°C for 30 min. The cells were rinsed three times and suspended in Ca^{2+}-free buffer. The fluorescence of the fura-2-loaded cells was measured by using CAF-110 spectrofluorometer (Jasco, Tokyo, Japan) with excitation at 340 and 380 nm, and emission at 510 nm. Elevation of the

intracellular Ca^{2+} concentration was evaluated as the increase in the ratio of fluorescence intensities at 340 nm and 380 nm (F340/F380).

Statistical analyses

All values are reported as means ± SEM. Statistical analyses of the differences in the means of experimental pairs were evaluated by the paired *t*-test. The *P* values obtained are indicated in the figure legends when statistically significant.

Results

Activation of p38 during cell isolation is suppressed by the addition of MCI-186

We previously showed that p38 was activated during cell isolation from parotid glands, which can be detected as an increase in its phosphorylation (17). We isolated acinar cells from rat parotid glands in the absence and presence of MCI-186. Phosphorylation of p38 was detected in the cells that were isolated without MCI-186 by immunoblotting (Fig. 2.1). In contrast, in cells isolated in the presence of MCI-186, the phosphorylated p38 was significantly decreased, although the amount of total p38 was not changed.

Maintenance of amylase activity and secretory granules in MCI-186-treated cells

To evaluate the degree of differentiation, we examined the activity of amylase, which is the most abundant salivary protein in parotid acinar cells. After 3 days of culture in the absence and presence of MCI-186, the cells were harvested and amylase activity was measured. Amylase activity is shown as the relative activity per mg of protein in the cell lysate.

Although the relative amylase activities of both cultured cells were lower than that in the cells just after isolation, MCI-186-treated cells have significantly higher activity than non-treated cells (1.5-fold, Fig. 2.2).

Salivary proteins like amylase are stored in SGs until stimulation. SGs are released via secretagogue-dependent exocytosis, which is an important function of exocrine cells. In primary culture, the acinar cells spread over the dish surface and formed a monolayer, and the number of SGs gradually decreased during culture (16). When SGs were labeled with an anti-amylase antibody at 3 days after isolation, the distribution of granules in the cells was not uniform (Fig. 2.3A); some cells had lost most of the granules, whereas other cells retained many granules. To compare the number of remaining granules in the non-treated and MCI-186-treated cells (Fig. 2.3A, B), we counted all the granules in the images (142.86 μm × 142.86 μm) of the confluent monolayer, and calculated the number of granules per unit area. MCI-186-treated cells retained more granules than the non-treated cells (1.7-fold, Fig. 2.3C). The difference in the number of granules between the two cultures was consistent with the remaining amylase activity.

Maintenance of stimulus-dependent amylase secretion in both the non-treated and MCI-186-treated cells

We cultured the cells in the absence and presence of isoproterenol (Iso) and collected the medium to measure the released amylase activity, which was determined as the percentage of the total activity in whole cells. A small amount of amylase was released without stimulation, and Iso enhanced the release from both non-treated and MCI-186-treated cells (Fig. 2.4). The addition of Iso increased amylase secretion in non-treated and MCI-168-treated cells 2.8-fold

and 3.0-fold, respectively. This enhancement was comparable to that observed in the cells just after isolation (15). Stimulus-dependent exocytosis capacity was not greatly impaired, even after 3 days of culture, although the synthesis of the amylase protein declined. MCI-168 did not promote the response to secretagogues, although it increased the number of remaining granules.

Enhancement of the elevation in the intracellular concentration Ca^{2+} in MCI-186-treated cells

Muscarinic stimulation increases the intracellular Ca^{2+} concentration ($[Ca^{2+}]_i$), which is essential for fluid secretion of saliva. Control cells isolated without MCI-186 responded to 10 μM carbachol (CCh). The rapid increase in $[Ca^{2+}]_i$ observed in the absence of extracellular Ca^{2+} indicates the release of Ca^{2+} from intracellular Ca^{2+} pool (Fig. 2.5A). The addition of extracellular Ca^{2+} (at a final concentration of 2.5 mM) induced an additional and sustained increase in $[Ca^{2+}]_i$, which corresponds to Ca^{2+} influx from the extracellular buffer. The CCh-dependent elevation in $[Ca^{2+}]_i$ was higher in MCI-186-treated cells than in the non-treated cells (Fig. 2.5A). The increase from the baseline to the peak F340/F380 was significantly higher in MCI-treated cells than in the non-treated cells (Fig. 2.5B).

Discussion

MCI-186 is a free radical scavenger that is widely used to treat ischemia brain damages and neurodegenerative diseases (21, 22). It is also thought to protect other organ systems such as

the cardiovascular system, and to suppress autoimmune disease (24-26). In this study, we showed that MCI-186 slightly improved the function of salivary acinar cells.

MCI-186 treatment suppressed the phosphorylation of p38. We previously reported that p38 phosphorylation is mediated by Src activation (17). Generation of ROS may be involved in Src activation since the NADPH oxidase inhibitor DPI suppressed activation of both Src and p38 (18). However, the viability of cultured cells at 24 h after cell isolation was decreased in the presence of DPI (data not shown). DPI may also inhibit enzymes that are essential for survival. In the presence of MCI-186, the cells survived and retained amylase-containing SGs. In general, primary cultures of exocrine cells rapidly lose their SGs (27, 28). In our primary culture system, the cells maintained the ability to generate SGs, nevertheless, the amount of amylase decreased to less than 10% of that in the cells just after isolation (about 60 units/mg of protein). In this study, the addition of MCI-186 increased amylase activity as well as the number of SGs. In contrast, amylase secretion was detected in both control and MCI-186-treated cells, and the enhancement of secretion induced by β-adrenergic stimulation was comparable to that observed in the cells just after isolation. Thus, during the generation of SGs, they may acquire the machinery required for stimulus-dependent exocytosis.

Muscarinic stimulation induces the secretion of water and ions from salivary acinar cells. Elevation of intracellular Ca^{2+}, mediated by the inositol triphosphate receptors IP_3R_2 and IP_3R_3, is essential for this secretion (1). The increase in the F340/F380 ratio induced by the addition of CCh in MCI-186-treated cells was significantly higher than the increase induced in non-treated cells. Based on this result, we expect that fluid secretion capacity will be more efficiently maintained in the presence of MCI-186. ROS production induced by

irradiation and inflammatory signals has been reported to reduce Ca^{2+} signaling in salivary gland cells. Irradiation induced the loss of STIM1, which is essential for Ca^{2+} influx from extracellular buffer and sustained intracellular Ca^{2+} elevation (29). A phosphodiesterase inhibitor, rolipram, which suppresses ROS production, enhanced CCh-induced Ca^{2+} signaling in submandibular gland cells (30). The cells were exposed to ROS during cell isolation from the glands, which may depress Ca^{2+} signaling. The presence of MCI-186 during cell isolation may have protected the cells from ROS and increased the CCh-induced Ca^{2+} response.

Although ROS has been reported to be involved in the impairment of salivary gland function in Sjögren's syndrome (19) and after irradiation (20), the intracellular signal pathways remain to be determined. In primary culture, ROS activated the Erk1/2-novel PKC pathway in addition to the Src-p38 pathway (31). We expect that multiple pathways also participate in the salivary gland dysfunction caused by irradiation and inflammation. We showed that γ-irradiation induced changes in the expression patterns of intercellular adhesion molecules *in vivo*, and similar changes were also observed in cultured acinar cells (32). Thus, we think that the responses triggered by cell isolation and by γ-irradiation have common properties.

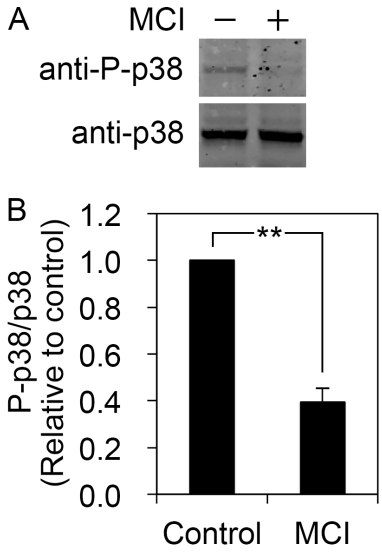

Fig. 2.1 Suppression of p38 activation by the addition of MCI-186.

(A) Immunoblotting analysis of lysates from non-treated (-) and MCI-186-treated (+) cells with antibodies against phosphorylated form (anti-P-p38) and total p38 (anti-p38). (B) Quantitative analysis of the immunoblots. After the intensity of immunoreactivity in MCI-treated sample (MCI) was normalized to that in non-treated sample (control) in the same blotting membrane, the ratio of the phosphorylated form to total p38 (P-p38/p38) was calculated in each experiment. Phosphorylation of p38 was significantly suppressed by the addition of MCI-186 (**$P < 0.01$, paired *t*-test, n = 4).

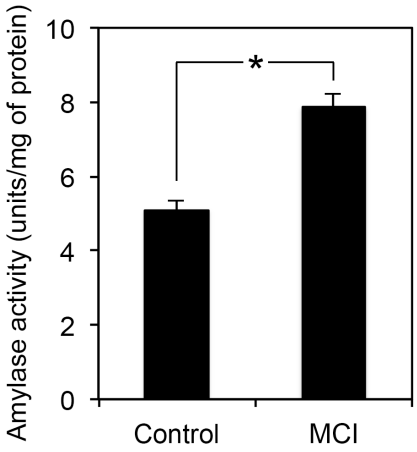

Fig. 2.2 Effect of MCI-186 on the decrease in relative amylase activity during culture. The relative amylase activity (units/mg of protein) in the lysates from non-treated (control) and MCI-186-treated (MCI) cells after 3 days of culture are shown. Although the relative amylase activity was lower than that in the cells just after isolation, the addition of MCI-186 suppressed the decrease in amylase activity (*$P < 0.05$, paired *t*-test, n = 4).

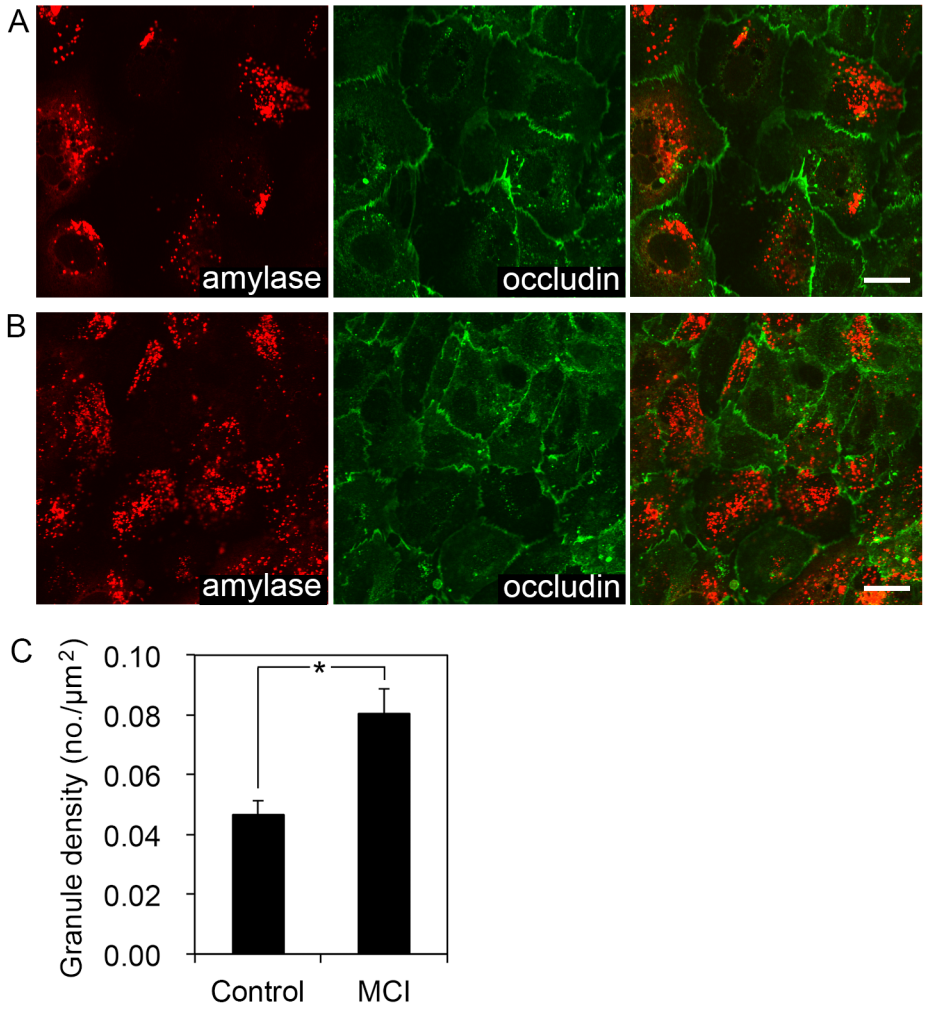

Fig. 2.3 Effect of MCI-186 on the number of secretory granules retained in the cultured acinar cells.

Immunofluorescence microscopy of non-treated (A) and MCI-186-treated (B) cells labeled with anti-amylase (red) and anti-occludin (green) antibodies. Optical sections were taken along the z-axis at 0.5 μm intervals, and the images shown are single z-planes. Spots labeled with the anti-amylase antibody correspond to secretory granules (SGs). A tight junction protein occludin was labeled in order to show the cell circumference. Bars, 20 μm. (C) Quantitative analysis of the density of SGs in the cells. Values are the number of granules per unit area. MCI-186-treated cells retained significantly more granules than the non-treated (control) cells (*$P < 0.05$, *t*-test, n = 8).

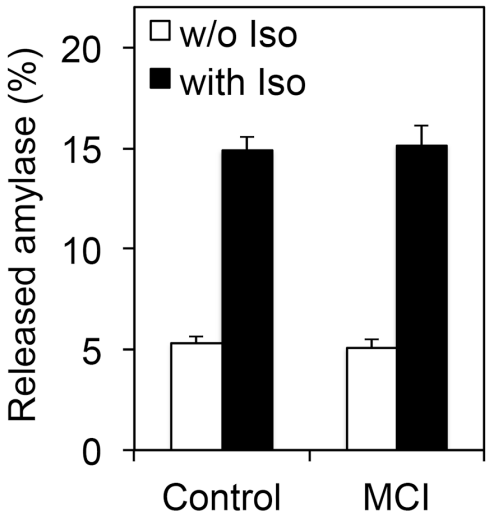

Fig. 2.4 Response of cultured acinar cells to β-adrenergic stimulation.

At 3 days after cell isolation, cultured acinar cells were incubated with or without (w/o) 10^{-6} M isoproterenol (Iso) at 37°C for 15 min. Amylase activity in the medium and cell lysate was measured, and the amount of released amylase is shown as a percentage of the total amylase. There was no significant difference between non-treated (control) and MCI-186-treated (MCI) cells (n = 4, paired t-test).

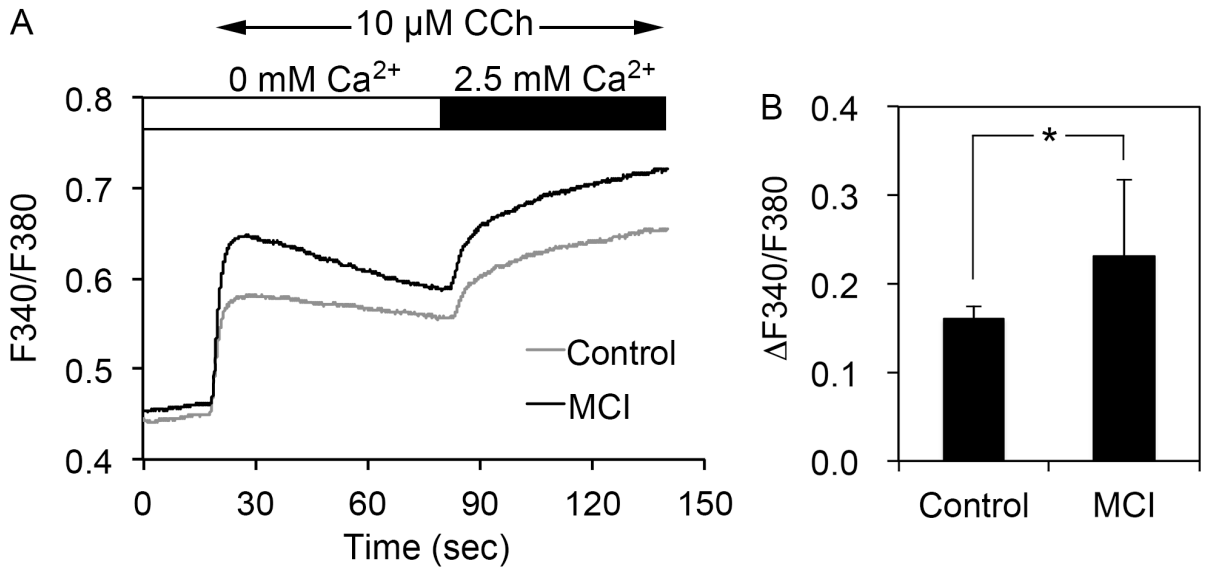

Fig. 2.5 Effect of MCI-186 on the calcium mobilization in isolated parotid acinar cells. (A) Cells were isolated from parotid glands in the absence (control) and presence (MCI) of MCI-186 and the freshly isolated cells were loaded with fura-2. Cells suspended in Ca^{2+}-free buffer (0 mM Ca^{2+}) were stimulated with 10 μM carbachol (CCh), and then 2.5 mM Ca^{2+} was added to the extracellular buffer. The values are shown as the ratio of the fluorescence intensities at 510 nm following excitation at 340 nm and 380 nm (F340/F380). (B) The increases in the F340/F380 ratio from the baseline to the peak response to CCh (ΔF340/F380) were compared. The response to CCh in the MCI-186-treated cells was significantly higher than the response in the control cells (*$P < 0.05$, paired *t*-test, n = 4).

Conclusion

MCI-186 improves both the Ca^{2+} response and protein exocytosis in salivary acinar cells by inhibiting Src-p38 signaling. Although the effect of MCI-186 was small, salivary acinar cells have the potential to recover from dysfunction *in vivo* if the damage is not too severe. For example, the secretory function of salivary glands is temporarily impaired by γ-irradiation, but is restored after several months when the radiation doses are lower (33). MCI-186 may increase the threshold for irreversible dysfunction. To protect the ability of Ca^{2+} response from tissue damages may be effective for maintenance of saliva secretion. In addition, there is a difference in Ca^{2+} mobilization between the two mouse strains that have a different ability to secrete saliva. To clarify the molecular mechanism that makes the difference may be useful to understand the cause of hyposalivation in xerostomia patients and to get a clue for recovery of secretory functions.

References

1. Futatsugi A, Nakamura T, Yamada MK, Ebisui E, Nakamura K, Uchida K, Kitaguchi T, Takahashi-Iwanaga H, Noda T, et al.: IP3 receptor types 2 and 3 mediate exocrine secretion underlying energy metabolism. Science, 309: 2232-4, 2005.
2. Caputo A, Caci E, Ferrera L, Pedemonte N, Barsanti C, Sondo E, Pfeffer U, Ravazzolo R, Zegarra-Moran O, et al.: TMEM16A, a membrane protein associated with calcium-dependent chloride channel activity. Science, 322: 590-4, 2008.
3. Yang YD, Cho H, Koo JY, Tak MH, Cho Y, Shim WS, Park SP, Lee J, Lee B, et al.: TMEM16A confers receptor-activated calcium-dependent chloride conductance. Nature, 455: 1210-5, 2008.
4. Schroeder BC, Cheng T, Jan YN, Jan LY: Expression cloning of TMEM16A as a calcium-activated chloride channel subunit. Cell, 134: 1019-29, 2008.
5. Turner RJ. Ion transport related to fluid secretion in salivary glands. In: Dobrosielski-Vergona K, editor. *Biology of the salivary glands*. Boca Raton, FL: CRC Press, Inc.; 1993. pp. 105-25.
6. Putney JW, Jr.: A model for receptor-regulated calcium entry. Cell Calcium, 7: 1-12, 1986.
7. Ong HL, de Souza LB, Zheng C, Cheng KT, Liu X, Goldsmith CM, Feske S, Ambudkar IS: STIM2 enhances receptor-stimulated Ca^{2+} signaling by promoting recruitment of STIM1 to the endoplasmic reticulum-plasma membrane junctions. Sci Signal, 8: ra3, 2015.
8. Liou J, Kim ML, Heo WD, Jones JT, Myers JW, Ferrell JE, Jr., Meyer T: STIM is a Ca^{2+} sensor essential for Ca^{2+}-store-depletion-triggered Ca^{2+} influx. Curr Biol, 15: 1235-41, 2005.

9. Roos J, DiGregorio PJ, Yeromin AV, Ohlsen K, Lioudyno M, Zhang S, Safrina O, Kozak JA, Wagner SL, et al.: STIM1, an essential and conserved component of store-operated Ca^{2+} channel function. J Cell Biol, 169: 435-45, 2005.

10. Yeromin AV, Zhang SL, Jiang W, Yu Y, Safrina O, Cahalan MD: Molecular identification of the CRAC channel by altered ion selectivity in a mutant of Orai. Nature, 443: 226-9, 2006.

11. Suzuki T: Caries susceptibility of mice of different strains infected with Streptococcus mutans. Jpn J Ped Dent, 198-203, 1985.

12. Endo C, Yamamoto S, Shimizu k: Study on factors that affect caries susceptibility in mice. Ped Dent J, 24: 39-45, 2014.

13. Tojyo Y, Tanimura A, Matsumoto Y: Evidence that substance-P receptors do not exist in mouse parotid and submandibular acinar cells. Arch Oral Biol, 38: 269-71, 1993.

14. Lytton J, Westlin M, Hanley MR: Thapsigargin inhibits the sarcoplasmic or endoplasmic reticulum Ca-ATPase family of calcium pumps. J Biol Chem, 266: 17067-71, 1991.

15. Fujita-Yoshigaki J, Tagashira A, Yoshigaki T, Furuyama S, Sugiya H: A primary culture of parotid acinar cells retaining capacity for agonists-induced amylase secretion and generation of new secretory granules. Cell Tissue Res, 320: 455-64, 2005.

16. Qi B, Fujita-Yoshigaki J, Michikawa H, Satoh K, Katsumata O, Sugiya H: Differences in claudin synthesis in primary cultures of acinar cells from rat salivary gland are correlated with the specific three-dimensional organization of the cells. Cell Tissue Res, 329: 59-70, 2007.

17. Fujita-Yoshigaki J, Matsuki-Fukushima M, Sugiya H: Inhibition of Src and p38 MAP kinases suppresses the change of claudin expression induced on dedifferentiation of

primary cultured parotid acinar cells. Am J Physiol Cell Physiol, 294: C774-85, 2008.

18. Moriyama S, Yokoyama M, Katsumata-Kato O: Enhancement of Src family kinase activity is essential for p38 MAP kinase-mediated dedifferentiation signal of parotid acinar cells. Int J Oral-Med Sci, 14: 33-40, 2015.

19. Ryo K, Yamada H, Nakagawa Y, Tai Y, Obara K, Inoue H, Mishima K, Saito I: Possible involvement of oxidative stress in salivary gland of patients with Sjögren's syndrome. Pathobiology, 73: 252-60, 2006.

20. Tai Y, Inoue H, Sakurai T, Yamada H, Morito M, Ide F, Mishima K, Saito I: Protective effect of lecithinized SOD on reactive oxygen species-induced xerostomia. Radiat Res, 172: 331-8, 2009.

21. Houkin K, Nakayama N, Kamada K, Noujou T, Abe H, Kashiwaba T: Neuroprotective effect of the free radical scavenger MCI-186 in patients with cerebral infarction: clinical evaluation using magnetic resonance imaging and spectroscopy. J Stroke Cerebrovasc Dis, 7: 315-22, 1998.

22. Abe K, Itoyama Y, Sobue G, Tsuji S, Aoki M, Doyu M, Hamada C, Kondo K, Yoneoka T, et al.: Confirmatory double-blind, parallel-group, placebo-controlled study of efficacy and safety of edaravone (MCI-186) in amyotrophic lateral sclerosis patients. Amyotroph Lateral Scler Frontotemporal Degener, 15: 610-7, 2014.

23. Fujita-Yoshigaki J: Analysis of changes in the expression pattern of claudins using salivary acinar cells in primary culture. Methods Mol Biol, 762: 245-58, 2011.

24. Nimata M, Okabe TA, Hattori M, Yuan Z, Shioji K, Kishimoto C: MCI-186 (edaravone), a novel free radical scavenger, protects against acute autoimmune myocarditis in rats. Am J Physiol Heart Circ Physiol, 289: H2514-8, 2005.

25. Arii K, Kumon Y, Sugahara K, Nakatani K, Ikeda Y, Suehiro T, Hashimoto K: Edaravone inhibits collagen-induced arthritis possibly through suppression of nuclear factor-kappa B. Mol Immunol, 45: 463-9, 2008.

26. Ji L, Liu Y, Zhang Y, Chang W, Gong J, Wei S, Li X, Qin L: The antioxidant edaravone prevents cardiac dysfunction by suppressing oxidative stress in type 1 diabetic rats and in high-glucose-induced injured H9c2 cardiomyoblasts. Can J Physiol Pharmacol, 94: 996-1006, 2016.

27. Fernandez NA, Liang T, Gaisano HY: Live pancreatic acinar imaging of exocytosis using syncollin-pHluorin. Am J Physiol Cell Physiol, 300: C1513-23, 2011.

28. Nicke B, Tseng MJ, Fenrich M, Logsdon CD: Adenovirus-mediated gene transfer of RasN17 inhibits specific CCK actions on pancreatic acinar cells. Am J Physiol, 276: G499-506, 1999.

29. Liu X, Gong B, de Souza LB, Ong HL, Subedi KP, Cheng KT, Swaim W, Zheng C, Mori Y, et al.: Radiation inhibits salivary gland function by promoting STIM1 cleavage by caspase-3 and loss of SOCE through a TRPM2-dependent pathway. Sci Signal, 10: eaa14064, 2017.

30. Lee DU, Shin DM, Hong JH: The regulatory role of rolipram on inflammatory mediators and cholinergic/adrenergic stimulation-induced signals in isolated primary mouse submandibular gland cells. Mediators Inflamm, 2016: 3745961, 2016.

31. Inoue D, Yokoyama M, Katsumata-Kato O: Tissue injury-induced reactive oxygen species cause dysfunction of parotid acinar cells via Erk-novel PKC activation. Int J Oral-Med Sci, 13: 6-11, 2014.

32. Yokoyama M, Narita T, Sakurai H, Katsumata-Kato O, Sugiya H, Fujita-Yoshigaki J:

Maintenance of claudin-3 expression and the barrier functions of intercellular junctions in parotid acinar cells via the inhibition of Src signaling. Arch Oral Biol, 81: 141-50, 2017.

33. Li Y, Taylor JM, Ten Haken RK, Eisbruch A: The impact of dose on parotid salivary recovery in head and neck cancer patients treated with radiation therapy. Int J Radiat Oncol Biol Phys, 67: 660-9, 2007.